# Sequential recognition of discrete export signals in flagellar subunits during bacterial Type III secretion


## Authors

Owain J. Bryant[a,b], Paraminder Dhillon[a,c], Colin Hughes[a], Gillian M. Fraser[a,*]

## Affiliations

[a]Department of Pathology, University of Cambridge, Tennis Court Road, Cambridge, CB2 1QP, United Kingdom

[b]Current address: Department of Biochemistry, University of Oxford, South Parks Road, Oxford, OX1 3QU

[c]Current address: The FEBS Journal Editorial Office, 59 St Andrew's House, Cambridge, CB2 3BZ, United Kingdom

## Corresponding author

[*]Gillian M. Fraser

Department of Pathology, University of Cambridge, Tennis Court Road, Cambridge, CB2 1QP, United Kingdom

Phone: +44 1223 330245

Email: gmf25@cam.ac.uk



## Keywords

Type III secretion system; protein export; bacterial flagella biogenesis

## Abstract

Type III Secretion Systems (T3SS) deliver subunits from the bacterial cytosol to nascent cell surface flagella. Early flagellar subunits that form the rod and hook substructures are unchaperoned and contain their own export signals. A gate recognition motif (GRM) docks subunits at the FlhBc component of the FlhAB-FliPQR export gate, but the gate must then be opened and subunits unfolded to pass into the flagellar channel. This induced us to seek further export signals in the subunits. Here, we identify a second signal at the extreme N-terminus of flagellar rod and hook subunits and determine that key to the signal is its hydrophobicity. We show that the two export signal elements are recognised separately and sequentially, as the N-terminal signal is recognised by the flagellar export machinery only after subunits have docked at $FlhB_C$ *via* the GRM. The position of the N-terminal hydrophobic signal in the subunit sequence relative to the GRM appeared to be important, as a FlgD deletion variant ($FlgD_{short}$), in which the distance between the N-terminal signal and the GRM was shortened, 'stalled' at the export machinery and was not exported. The attenuation of motility caused by $FlgD_{short}$ was suppressed by mutations that destabilised the closed conformation of the FlhAB-FliPQR flagellar export gate, suggesting that the hydrophobic N-terminal signal might trigger opening of the gate.

## Introduction

Type III Secretion Systems (T3SS) are multi-component molecular machines that deliver protein cargo from the bacterial cytosol either to their site of assembly in cell surface flagella or virulence factor injectosomes, or directly to their site of action in

eukaryotic target cells or the extracellular environment [1-5]. The flagellar T3SS (fT3SS) directs the export of thousands of structural subunits required for the assembly and operation of flagella, rotary nanomotors for cell motility that extend from the bacterial cell surface [1],[6]. Newly synthesised subunits of the flagellar rod, hook and filament are targeted to the fT3SS, where they are unfolded and translocated across the cell membrane, powered by the proton motive force and ATP hydrolysis, into an external export channel that spans the length of the nascent flagellum [7],[8]. During flagellum biogenesis, when the rod/hook structure reaches its mature length, the fT3SS switches export specificity from recognition of 'early' rod/hook subunits to 'late' subunits for filament assembly [9],[10]. This means that early and late flagellar subunits must be differentiated by the fT3SS machinery to ensure that they are exported at the correct stage of flagellum biogenesis. This is achieved, in part, by targeting subunits to the export machinery at the right time using a combination of export signals in the subunit mRNA and/or polypeptide. T3SS substrates contain N-terminal signals for targeting to the export machinery, however they do not share a common peptide sequence [11-15]. In addition, some substrates are piloted to the T3SS machinery by specific chaperones [16-21].

The core export components of the fT3SS are evolutionarily related to those of the virulence injectosome, with which they share considerable structural and amino acid sequence similarity [22-25]. The flagellar export machinery comprises an ATPase complex (FliHIJ) located in the cytoplasm, peripheral to the membrane. Immediately above the ATPase is a nonameric ring formed by the cytoplasmic domain of FlhA ($FlhA_C$), which functions as a subunit docking platform [20],[21],[26]. A recent cryo-

ET map indicates that the FlhA family have a sea-horse-like structure, in which FlhAc forms the ‘body’ and the FlhA N-terminal region ($FlhA_N$) forms the ‘head’, which is fixed in the plane of the membrane [27]. $FlhA_N$ wraps around the base of a complex formed by FliPQR and the N-terminal sub-domain of FlhB ($FlhB_N$), and together these form the FlhAB-FliPQR export gate that connects the cytoplasm to the central channel in the nascent flagellum, which is contiguous with the extracellular environment [22],[28]. $FlhB_N$ is connected *via* a linker ($FlhB_{CN}$) to the cytoplasmic domain of FlhB ($FlhB_C$), which is thought to sit between the $FlhA_N$ and $FlhA_C$ rings, where it functions as a docking site for early flagellar subunits [22],[14],[28].

The ‘early’ flagellar subunits that assemble to form the rod and hook substructures are not chaperoned: instead, the signals for targeting and export are found within the early subunits themselves. We have shown that one of these signals is a small hydrophobic sequence termed the gate recognition motif (GRM), which is essential for early subunit export [14]. This motif binds a surface exposed hydrophobic pocket on FlhBc [14]. Once subunits reach the export machinery, they must be unfolded before they can pass through the narrow channel formed by FliPQR-$FlhB_N$ into the central channel of the nascent flagellum, through which the subunits transit until they reach the tip and fold into the structure [22],[6]. Structural studies suggest that FliPQR-$FlhB_N$ adopts an energetically favourable closed conformation, possibly to maintain the membrane permeability barrier [22],[25],[29],[30]. This suggests that there must be a mechanism to trigger opening of the export gate when subunits dock at cytoplasmic face of the flagellar export machinery.

73 Here we sought to identify new export signals within flagellar rod/hook subunits,
74 using the hook-cap subunit FlgD as a model export substrate. We show that the
75 extreme N-terminus of rod/hook subunits contains a hydrophobic export signal and
76 investigate its functional relationship to the subunit gate recognition motif (GRM).
77

78 **Results**

79 ***Identification of a hydrophobic export signal at the N-terminus of FlgD***

80 The N-terminal region of flagellar rod and hook subunits is required for their export
81 [12],[14]. Using the flagellar hook-cap protein FlgD as a model rod/hook subunit, we
82 sought to identify specific export signals within the N-terminus. A screen of ten FlgD
83 variants containing internal five-residue scanning deletions in the first 50 residues
84 (though FlgDΔ2-5 is a four-residue deletion, retaining the initial methionine) identified
85 just two variants defective for export into culture supernatant (**Fig. 1A**). Loss of
86 residues 2-5 caused a significant reduction in export, as did deletion of residues 36-
87 40, though to a lesser extent (**Fig. 1A**; [14]). We have shown that FlgD residues 36-
88 40 are the gate recognition motif (GRM) required for transient subunit docking at the
89 $FlhB_C$ component of the export gate [14]. The results suggest that the extreme N-
90 terminus might also be important for interaction with the export machinery.
91

92 To gain insight into the putative new signal, we screened for intragenic suppressor
93 mutations that could restore export of the FlgDΔ2-5 variant. A *Salmonella flgD* null
94 strain expressing *flgD*Δ2-5 *in trans* was inoculated into soft-tryptone agar and
95 incubated until 'spurs' of motile cell populations appeared. Sequencing of *flgD*Δ2-5

96 alleles from these motile populations identified ten different intragenic gain-of-
97 function mutations. These could be separated into two classes (**Fig. 1B**).
98
99 The first class of motile revertants carried *flgD*Δ2-5 alleles with missense mutations
100 that introduced small non-polar residues at the extreme N-terminus of FlgDΔ2-5 (**Fig.**
101 **1B**). Deletion of residues 2-5 ($^{2}$SIAV$^{5}$) had removed all small non-polar amino acids
102 from the first ten residue region of FlgD, effectively creating a new N-terminus
103 containing a combination of polar, charged or large non-polar residues (**Fig. S1**).
104 Analysis of other flagellar rod and hook subunit primary sequences revealed that in
105 every case their native N-terminal regions contain small non-polar residues
106 positioned upstream of the gate recognition motif (GRM residues 36-40; **Fig. S1**),
107 indicating that hydrophobicity may be key to the function of the N-terminal export
108 signal. Export assays performed with two representative motile revertant strains
109 carrying *flgDΔ2-5* variants with gain-of-function point mutations, those encoding
110 FlgDΔ2-5-$N_8$I and FlgDΔ2-5-$T_{11}$I, revealed that export of these subunits had
111 recovered to ~50% of the level observed for wild type FlgD (**Fig. 1C**; **Fig. S2; Fig.**
112 **S3**).
113
114 The second class of motile revertants carried *flgD*Δ2-5 alleles that had acquired
115 duplications or insertions introducing at least six additional residues between the
116 FlgDΔ2-5 N-terminus and the gate recognition motif (GRM; **Fig. 1B**). It seemed
117 possible that these insertions/duplications might have restored subunit export either
118 by insertion of amino acids that could function as a 'new' hydrophobic export signal,

119 or by restoring the position of an existing small hydrophobic residue or sequence
120 relative to the GRM.
121
122 To assess these possibilities, we tested whether export of FlgDΔ2-5 could be
123 recovered by inserting either polar ($^{19}$STSTST$^{20}$) or small non-polar ($^{19}$AGAGAG$^{20}$)
124 residues in the FlgDΔ2-5 N-terminal region at a position equivalent to one of the
125 suppressing duplications ($^{19}$GSGSMT$^{20}$; **Fig. 1B and D**; **Fig. S3**). We reasoned that
126 if suppression by the additional sequence had been caused by repositioning an
127 existing small hydrophobic amino acid relative to the GRM, then any insertional
128 sequence (polar or non-polar) would restore export, while if suppression had resulted
129 from insertion of a 'new' export signal, then either the polar STSTST or non-polar
130 AGAGAG, but not both, could be expected to restore export.
131
132 We found that both the engineered FlgD variants (FlgDΔ2-5-$^{19}$AGAGAG$^{20}$ and
133 FlgDΔ2-5-$^{19}$STSTST$^{20}$) were exported from a *Salmonella flgD* null strain as
134 effectively as the gain-of-function mutant FlgDΔ2-5-$^{19}$GSGSMT$^{20}$ isolated from the
135 suppressor screen (**Fig. 1D**). This suggests that the insertions had repositioned a
136 sequence in the FlgDΔ2-5 N-terminus relative to the GRM to overcome the loss of
137 small hydrophobic residues.
138
139 ***The position of the hydrophobic export signal relative to the gate recognition***
140 ***motif is critical for rod and hook subunit export***
141 The intragenic suppressor experiments indicated that FlgD export requires a
142 hydrophobic export signal towards the N-terminus and that the position of this

143 hydrophobic signal relative to the previously described GRM is important. Sequence
144 analysis of the gain-of-function FlgDΔ2-5 insertion variants revealed that the
145 insertions were all located between the GRM and valine$_{15}$ ($V_{15}$; **Fig. 1B**). We
146 reasoned that they repositioned valine$_{15}$ relative to the GRM, such that it could
147 perform the function of the N-terminal hydrophobic signal lost in FlgDΔ2-5. To test
148 this view, we replaced $V_{15}$ with alanine in the gain-of-function variant FlgDΔ2-5-
149 $^{19}$(GSGSMT)$^{20}$ and assayed its export in the *Salmonella flgD* null (**Fig. 2A**; **Fig. S4**).
150 Unlike the *flgD* null strain producing either the parental FlgDΔ2-5-$^{19}$(GSGSMT)$^{20}$ or
151 wild type FlgD, the *flgD* null carrying variant FlgDΔ2-5-$^{19}$(GSGSMT)$^{20}$-$V_{15}$A was non-
152 motile, reflecting the variant's failure to export (**Fig. 2A**). This suggests that the $V_{15}$
153 residue had indeed compensated for the missing N-terminal hydrophobic signal.
154
155 By screening for intragenic suppressors of the motility defect associated with
156 FlgDΔ2-5-$^{19}$(GSGSMT)$^{20}$-$V_{15}$A, four gain-of-function missense mutations were
157 identified, $M_7$I, $D_9$A, $T_{11}$I and $G_{14}$V. All of these had introduced small hydrophobic
158 residues, all positioned at least 27 residues upstream of the GRM. These FlgDΔ2-5-
159 $^{19}$(GSGSMT)$^{20}$-$V_{15}$A gain-of-function variants restored motility to the *Salmonella flgD*
160 null strain and were exported at levels similar to wildtype FlgD and FlgDΔ2-5-
161 $^{19}$(GSGSMT)$^{20}$ (**Fig. 2A**). These data confirm the importance of small non-polar
162 residues positioned upstream of the GRM.
163
164 Our results so far had indicated that the position of the FlgD N-terminal hydrophobic
165 export signal relative to the GRM was critical and suggested that, for export to occur
166 efficiently, at least 26 residues must separate the hydrophobic signal and the GRM

167 (**Fig 1C**). In the primary sequences of all *Salmonella* flagellar rod/hook subunits the
168 GRM is positioned ≥ 30 amino acids downstream of the subunit N-terminus (**Fig S1**),
169 suggesting that separation of the two signals by a minimum number of residues
170 might be a common feature among early flagellar subunits. To test this, a suite of
171 engineered *flgD* alleles was constructed that encoded FlgD variants in which
172 wildtype residues 9-32 were replaced with between one and four repeats of the six
173 amino acid sequence Gly-Ser-Thr-Asn-Ala-Ser (GSTNAS). Swimming motility and
174 export assays revealed that the minimum number of inserted GSTNAS repeats that
175 could support efficient FlgD export was three, equivalent to separation of the
176 hydrophobic N-terminal signal and the GRM by 24 residues (**Fig. 2B**; **Fig. S5**).
177 Below this threshold, FlgD export and swimming motility were strongly attenuated
178 (**Fig. 2B**). A further set of recombinant *flgD* alleles was constructed, which encoded
179 FlgDΔ9-32 variants carrying two GSTNAS repeats (hereafter termed $FlgD_{short}$)
180 directly followed by between one and five additional residues (**Fig. 2C**; **Fig. S5**).
181 Motility and FlgD export increased incrementally with the addition of each amino acid
182 (**Fig. 2C**). The data indicate that a low level of FlgD export is supported when the
183 hydrophobic N-terminal signal ($_{2}SIAV_{5}$) and the GRM ($_{36}FLTLL_{40}$) are separated by
184 19 residues, with export efficiency and swimming motility increasing as separation of
185 the export signals approaches the optimal 30 residues.
186
187 To further establish the requirement for a minimum number of residues between the
188 hydrophobic N-terminal signal and the GRM, we screened for intragenic suppressor
189 mutations that could restore swimming motility in a *flgD* null strain producing
190 $FlgD_{short}$. Sequencing of $flgD_{short}$ alleles from motile revertant strains identified 12

191 gain-of-function mutations that introduced additional residues between the
192 hydrophobic N-terminal signal and the GRM (**Fig. S6**). Swimming motility and FlgD
193 export was assessed for three *flgD* null strains expressing representative *flgD*$_{short}$
194 gain-of-function variants and all showed increased FlgD subunit export and
195 swimming motility compared to the *flgD* null expressing *flgD*$_{short}$ (**Fig. 2D**; **Fig. S6**).
196 The data confirm that the position of the hydrophobic N-terminal signal relative to the
197 GRM is critical for efficient FlgD subunit export.
198
199 To establish that this is a general requirement for the export of other rod and hook
200 subunits, engineered alleles of *flgE* (hook) and *flgG* (rod) were constructed that
201 encoded variants in which FlgE residues 9-32 or FlgG residues 11-35 were either
202 deleted (FlgE$_{short}$ and FlgG$_{short}$) or replaced with four repeats of the sequence
203 GSTNAS (**Fig. 3**; **Fig. S7**). As had been observed for FlgD$_{short}$, export of the
204 FlgE$_{short}$ and FlgG$_{short}$ variants was severely attenuated compared to wild type FlgE
205 and FlgG (**Fig. 3**). Furthermore, insertion of four GSTNAS repeats into FlgE$_{short}$ and
206 FlgG$_{short}$ recovered subunit export to wild type levels, indicating that the minimum
207 separation of the hydrophobic N-terminal signal and the GRM is a feature throughout
208 rod and hook subunits (**Fig. 3**).
209
210 ***Sequential engagement of the subunit GRM and hydrophobic N-terminal***
211 ***export signal by the flagellar export machinery***
212 Having identified a new hydrophobic N-terminal export signal and established that its
213 position relative to the GRM was critical, we next wanted to determine the order in
214 which the signals were recognised/engaged by the export machinery. The signals

215 might be recognised simultaneously, with both being required for initial entry of
216 rod/hook subunits into the export pathway. Alternatively, they might be recognised
217 sequentially. If this were the case, then a subunit variant that possessed the 'first'
218 signal but was deleted for the 'second' signal might enter the export pathway but fail
219 to progress, becoming stalled at a specific step to block the pathway and prevent
220 export of wild type subunits. To test if FlgDΔ2-5 or FlgDΔGRM stalled in the export
221 pathway, recombinant expression vectors encoding these variants or wild type FlgD
222 were introduced into a *Salmonella* Δ*recA* strain that is wild type for flagellar export
223 (**Fig. 4**). We could then assess whether the variant FlgD constructs could interfere *in*
224 *trans* with the wild type flagellar export. We saw that FlgDΔ2-5 inhibited motility and
225 export of the FliK and FlgK flagellar subunits, whereas FlgDΔGRM did not (**Fig. 4B**
226 **and C**). The data indicate that FlgDΔ2-5 enters the flagellar export pathway and
227 stalls at a critical point, blocking export. In contrast, FlgDΔGRM does not stall or
228 block export.
229
230 To determine whether FlgDΔ2-5 stalls at a point before or after subunit docking at
231 the $FlhB_C$ component of the flagellar export gate *via* the GRM, a recombinant vector
232 encoding a FlgD variant in which both export signals were deleted (FlgDΔ2-5ΔGRM)
233 was constructed. If loss of the hydrophobic N-terminal signal had caused subunits to
234 stall after docking at $FlhB_C$, then additional deletion of the subunit GRM would relieve
235 this block. Motility and subunit export assays revealed that the *Salmonella* Δ*recA*
236 strain producing FlgDΔ2-5ΔGRM displayed swimming motility and levels of FliK and
237 FlgK subunit export similar to cells producing FlgDΔGRM (**Fig. 4B and C**). The data

238 suggest that FlgDΔ2-5 stalls after docking at the $FlhB_C$ export gate, preventing
239 docking of other early subunits.
240
241 It seemed possible that subunit docking *via* the GRM to the $FlhB_C$ export gate might
242 position the hydrophobic N-terminal signal in close proximity to its recognition site on
243 the export machinery. If this were the case, 'short' subunit variants containing
244 deletions that decreased the number of residues between the hydrophobic N-
245 terminal signal and the GRM might also stall at $FlhB_C$, and this stalling might be
246 relieved by additional deletion of the GRM. To test this, recombinant expression
247 vectors encoding 'short' subunit variants ($FlgE_{short}$ or $FlgD_{short}$), 'short' subunit
248 variants additionally deleted for the GRM ($FlgE_{short}$ΔGRM or $FlgD_{short}$ΔGRM) or wild
249 type FlgE or FlgD were introduced into a *Salmonella* Δ*recA* strain (**Fig 5**). Compared
250 to the wild type subunits expressed *in trans*, the 'short' subunits inhibited swimming
251 motility and the export of other flagellar subunits (FliD, FliK, FlgK), whereas
252 $FlgE_{short}$ΔGRM and $FlgD_{short}$ΔGRM did not (**Fig 5**). Taken together with the data
253 presented in Figure 4, the results indicate that the subunit GRM and the hydrophobic
254 N-terminal signal are recognised sequentially, with subunits first docking at $FlhB_C$ *via*
255 the GRM, which positions the hydrophobic N-terminal signal for subsequent
256 interactions with the export machinery (**Fig 4D**).
257
258 **Mutations that promote opening of the export gate partially compensate for**
259 **incorrect positioning of the N-terminal export signal**
260 The accruing data indicated that subunit docking at $FlhB_C$ might correctly position the
261 hydrophobic N-terminal signal for recognition by the export machinery. To model the

262 position of $FlhB_C$ relative to other components of the export machinery, we placed
263 the structures of $FlhB_C$ and the FliPQR-$FlhB_N$ export gate into the tomographic
264 reconstruction of the *Salmonella* SPI-1 type III secretion system (**Fig 6B**; [31]). The
265 model indicated that FliPQR-$FlhB_N$ and the subunit docking site on $FlhB_C$ are
266 separated by a minimum distance of ~78 Å, and that $FlhB_C$ is positioned no more
267 than ~22-45 Å from FlhA (Fig 6A; [27]). Taking FlgD as a model early flagellar
268 subunit, the distance between the FlgD N-terminal hydrophobic signal and the GRM
269 was found to be in the range of ~45 Å ($\alpha$-helix) to ~105 Å (unfolded contour length),
270 depending on the predicted structure adopted by the subunit N-terminus (Fig 6A).
271 Based on these estimates, it seemed feasible that the hydrophobic N-terminal signal
272 of a subunit docked at $FlhB_C$ could contact either FlhA or the FliPQR-$FlhB_N$ complex,
273 and that this interaction might trigger opening of the export gate [27],[30],[22]. If this
274 were true, mutations that promote the open conformation of the export gate might
275 compensate for the incorrect positioning of the hydrophobic N-terminal export signal
276 in 'short' rod/hook subunits. One such export gate mutation, FliP-$M_{210}$A, has been
277 shown to increase ion conductance across the bacterial inner membrane, indicating
278 that this gate variant fails to close efficiently [29].
279
280 To test whether the FliP-$M_{210}$A variant gate could promote export of 'short' subunits,
281 in which the distance between the hydrophobic N-terminal signal and the GRM was
282 reduced, a recombinant expression vector encoding $FlgD_{short}$ was introduced into
283 *Salmonella flgD* null strains in which the *fliP* gene had been replaced with
284 recombinant genes encoding either a functional FliP variant with an internal HA-tag
285 (designated wild type gate) or the equivalent HA-tagged FliP-$M_{210}$A variant

286 (designated $M_{210}A$ gate; **Fig. 6C**; **Fig. S8**). The swimming motility of these strains
287 was found to be consistently stronger in the strain producing the $M_{210}A$ gate
288 compared to the strain with the wild type gate, with the motility halo of the *fliP*-
289 M210A-Δ*flgD* strain expressing $FlgD_{short}$ having a 50% greater diameter than that of
290 the wild type *fliP*-Δ*flgD* strain expressing $FlgD_{short}$ (**Fig. 6D**). This increase in motility
291 indicated that the defect caused by incorrect positioning of the hydrophobic N-
292 terminal signal relative to the GRM in $FlgD_{short}$ could indeed be partially
293 compensated by promoting the gate open conformation.
294
295 **Discussion**
296 T3SS substrates contain N-terminal export signals, but these have not been fully
297 defined and how they promote subunit export remains unclear. Here, we
298 characterised a new hydrophobic N-terminal export signal in early flagellar rod/hook
299 subunits and showed that the position of this signal relative to the known subunit
300 gate recognition motif (GRM) is key to export.
301
302 Loss of the hydrophobic N-terminal signal in the hook cap subunit FlgD had a
303 stronger negative effect on subunit export than deletion of the GRM that enables
304 subunit docking at $FlhB_C$, suggesting that the hydrophobic N-terminal signal may be
305 required to trigger an essential export step. A suppressor screen showed that the
306 export defect caused by deleting the hydrophobic N-terminal signal could be
307 overcome by mutations that either reintroduced small non-polar amino acids
308 positioned 3-7 residues from the subunit N-terminus (*e.g.* $M_7I$), or introduced
309 additional residues between $V_{15}$ and the GRM. In such 'gain of function' strains

310 containing insertions, changing $V_{15}$ to alanine abolished subunit export, which was
311 rescued by re-introduction of small non-polar residues close to the N-terminus.
312 These data point to an essential export function for small non-polar residues close to
313 the N-terminus of rod/hook subunits.
314
315 It was fortuitous that we chose FlgD as the model for early flagellar subunit. All early
316 subunits contain small hydrophobic residues close to the N-terminus, but FlgD is
317 unique in that only four ($I_3$, $A_4$, $V_5$ and $V_{15}$) of its first 25 residues are small and non-
318 polar (**Fig. S1**). Indeed, there are only three other small hydrophobic residues
319 between the FlgD N-terminus and the GRM (**Fig. 1**). While deletion of residues 2-5 in
320 FlgD removes the critical hydrophobic N-terminal signal, similar deletions in the N-
321 terminal regions of other rod/hook subunits reposition existing small non-polar
322 residues close to the N-terminus (**Fig. S1**). This is perhaps why previous deletion
323 studies in early flagellar subunits have failed to identify the hydrophobic N-terminal
324 signal [14],[37],[38].
325
326 The finding that subunits lacking the hydrophobic N-terminal export signal, but not
327 the GRM, stalled during export suggested that these two signals were recognised by
328 the flagellar export machinery in a specific order. Mutant variants of other flagellar
329 export substrates or export components have been observed to block the export
330 pathway. For example, a FlgN chaperone variant lacking the C-terminal 20 residues
331 stalls at the FliI ATPase [39], while a GST-tagged FliJ binds FlhA but is unable to
332 associate correctly with FliI so blocking wild type FliJ interaction with FlhA [40].
333 These attenuations can be reversed by further mutations that disrupt the stalling

334 interactions. This was also observed for FlgDΔ2-5. Loss of the hydrophobic N-
335 terminal signal resulted in a dominant-negative effect on motility and flagellar export,
336 but this was abolished by subsequent deletion of the GRM. This indicates that
337 FlgDΔ2-5 stalls in the export pathway at $FlhB_C$, blocking the binding site for early
338 flagellar subunits. These data are consistent with sequential recognition of the two
339 export signals: the GRM first docking subunits at $FlhB_C$, and positioning the
340 hydrophobic N-terminal signal to trigger the next export step.
341
342 The position of the subunit hydrophobic N-terminal export signal relative to the GRM
343 appears critical for export. Engineering of *flgD* to encode variants in which the region
344 between the N-terminus and the GRM was replaced with polypeptide sequences of
345 varying lengths showed that these signals must be separated by a minimum of 19
346 residues for detectable export, with substantial export requiring separation by 30
347 residues (**Fig. 3**). When subunits dock at $FlhB_C$, which is likely situated within or just
348 below the plane of the inner membrane, the hydrophobic N-terminal signal is
349 positioned close to the FlhAB-FliPQR export gate (**Fig. 6B**). Subunits in which the
350 GRM and N-terminal signal are brought closer together stall at $FlhB_C$, suggesting
351 that the hydrophobic N-terminal signal is unable to contact its recognition site on the
352 export machinery (**Figs. 5, 6A and 6B**). In all flagellar rod/hook subunits, the GRM is
353 positioned at least 30 residues from the N-terminus (**Fig. S1**). The physical distance
354 between the two signals will depend on the structure adopted by the subunit N-
355 terminus (**Fig. 6A**). The N-terminal region of flagellar subunits is often unstructured
356 in solution [11-15],[32], and such disorder may be an intrinsic feature of flagellar
357 export signals [11-15],[33],[34], as they are typical in other bacterial export N-

358 terminal substrate signals such as those of the Sec and Tat systems [35],[36].
359 Unstructured signals may facilitate multiple interactions with different binding
360 partners during export, and in the case of export systems that transport unfolded
361 proteins they may aid initial entry of substrates into narrow export channels [35].
362
363 As yet, nothing is known about the structure of the subunit N-terminal domain upon
364 interaction with the flagellar export machinery. Signal peptides in TAT pathway
365 substrates switch between disordered and α-helical conformations depending on the
366 hydrophobicity of the environment [41]. It therefore seems likely that local
367 environments along the flagellar export pathway will influence the conformation of
368 subunit export signals [42],[22]. In flagellar subunits, if the region between the
369 hydrophobic N-terminal signal and the GRM is unstructured and extended, this
370 would correspond to a polypeptide contour length of approximately 72-105 Å (where
371 the length of one amino acid is ~3.6 Å). If the same region were to fold as an α-helix,
372 its length would be approximately 30-36 Å (where one amino acid rises every ~1.5
373 Å). Without further structural information on subunit interactions with the flagellar
374 export machinery and the precise position of $FlhB_C$ within the machinery, it is difficult
375 to determine precisely where the hydrophobic N-terminal signal contacts the
376 machinery.
377
378 We speculate that one function of the subunit hydrophobic N-terminal signal might
379 be to trigger opening of the FlhAB-FliPQR export gate, which rests in an
380 energetically favourable closed conformation to maintain the permeability barrier
381 across the bacterial inner membrane [29],[22],[30],[27]. The atomic resolution

382 structure of FliPQR showed that it contains three gating regions [22]. FliR provides a
383 loop (the R-plug) that sits within the core of the structure. Below this five copies of
384 FliP each provides three methionine residues that together form a methionine-rich
385 ring under which ionic interactions between FliQ residues hold the base of the
386 structure shut (Q-latch). If the function of the subunit hydrophobic N-terminal signal
387 was to trigger opening of this gate, we hypothesised that mutations which
388 destabilised the gate's closed conformation would suppress the motility defect
389 associated with $FlgD_{short}$, in which the distance between the N-terminal signal and
390 the GRM is reduced. Introduction of the FliP-$M_{210}$A mutation, which partially
391 destabilises the gate's closed state, did indeed partly suppress the $FlgD_{short}$ motility
392 defect. We did not find export gate variants that completely destabilised gate closure,
393 but it may be that such mutations disrupt the membrane permeability barrier [29].
394 This could also explain why in screens for suppressors of FlgDΔ2-5 or $FlgD_{short}$ we
395 did not isolate mutations in genes encoding export gate components (data not
396 shown).
397
398 The surface-exposed hydrophobic GRM-binding pocket on $FlhB_C$ is well conserved
399 across the T3SS SctU family, to which FlhB belongs [14],[43],[44]. Furthermore, the
400 GRM is conserved in all four injectosome early subunits (SctI, SctF, SctP, OrgC) and
401 is located at least 30 residues away from small hydrophobic residues near the
402 subunit N-terminus. It therefore seems plausible that the 'dual signal' mechanism we
403 propose for early flagellar export operates in all T3SS pathways.
404

405 In many other pathways, the presence of a substrate triggers opening or assembly of
406 the export channel. The outer membrane chitin transporter in *Vibrio* adopts a closed
407 conformation in which the N-terminus of a neighbouring subunit acts as a pore plug
408 [45]. Chitin binding to the transporter ejects the plug, opening the transport channel
409 and allowing chitin transport [45]. In the Sec pathway, interactions of SecA,
410 ribosomes or pre-proteins with SecYEG can induce conformational changes that
411 promote channel opening [46-48],[35]. In the TAT system, which transports folded
412 substrates across the cytoplasmic membrane, substrate binding to the TatBC
413 complex triggers association with, and subsequent polymerisation of, TatA, which is
414 required for substrate translocation [49],[36]. All of these mechanisms serve both to
415 conserve energy and prevent disruption of the membrane permeability barrier. Our
416 data suggest that in a comparable way the signal of non-polar residues within the N-
417 termini of early rod/hook subunits trigger export gate opening.

418 **Methods**

419 **Bacterial strains, plasmids and growth conditions**

420 *Salmonella* strains and plasmids used in this study are listed in **Supplementary**
421 **Table 1**. The Δ*flgD*::$K_m^R$ strain in which the *flgD* gene was replaced by a kanamycin
422 resistance cassette was constructed using the λ Red recombinase system [57].
423 Strains containing chromosomally encoded FliP variants were constructed by aph-I-
424 SceI Kanamycin resistance cassette replacement using pWRG730 [58].
425 Recombinant proteins were expressed in *Salmonella* from the isopropyl β-D-
426 thiogalactoside-inducible (IPTG) inducible plasmid pTrc99a [59]. Bacteria were
427 cultured at 30–37 °C in Luria-Bertani (LB) broth containing ampicillin (100 µg/ml).
428

429 **Flagellar subunit export assay**

430 *Salmonella* strains were cultured at 37 °C in LB broth containing ampicillin and IPTG
431 to mid-log phase ($OD_{600nm}$ 0.6-0.8). Cells were centrifuged (6000*g*, 3 min) and
432 resuspended in fresh media and grown for a further 60 min at 37 °C. The cells were
433 pelleted by centrifugation (16,000*g*, 5 min) and the supernatant passed through a 0.2
434 µm nitrocellulose filter. Proteins were precipitated with 10% trichloroacetic acid
435 (TCA) and 1% Triton-X100 on ice for 1 hour, pelleted by centrifugation (16,000*g*, 10
436 min), washed with ice-cold acetone and resuspended in SDS-PAGE loading buffer
437 (volumes calibrated according to cell densities). Fractions were analysed by
438 immunoblotting.
439
440
441

442 **Motility assays**

443 For swimming motility, cultures were grown in LB broth to A600nm 1. Two microliters
444 of culture were inoculated into soft tryptone agar (0.3% agar, 10 g/L tryptone, 5g/L
445 NaCl) containing ampicillin (100 µg/ml). Plates were incubated at 37 °C for between
446 4 and 6 hours unless otherwise stated.

447

448 **Isolation of motile strains carrying suppressor mutations**

449 Cells of the *Salmonella flgD* null strain transformed with plasmids expressing FlgD
450 variants (FlgDΔ2-5, FlgDΔ2-5-$^{19}$GSGSMT$^{20}$-V15A or FlgD$_{short}$) were cultured at 37
451 °C in LB broth containing ampicillin (100 µg/ml) to mid-log phase and inoculated into
452 soft tryptone agar (0.3% agar, 10 g/L tryptone, 5g/L NaCl) containing ampicillin (100
453 µg/ml). Plates were incubated at 30 °C until motile 'spurs' appeared. Cells from the
454 spurs were streaked to single colony and cultured to isolate the *flgD* encoding
455 plasmid. Plasmids were transformed into the *Salmonella flgD* null strain to assess
456 whether the plasmids were responsible for the motile suppressor phenotypes.
457 Plasmids were sequenced to identify the suppressor mutations.

458

459 **Quantification and statistical analysis**

460 Experiments were performed at least three times. Immunoblots were quantified using
461 Image Studio Lite. The unpaired two-tailed Student's *t*-test was used to determine *p*-
462 values and significance was determined as $*p < 0.05$. Data are represented as mean
463 ± standard error of the mean (SEM), unless otherwise specified and reported as
464 biological replicates.

465

466 **Author contributions**

467 **Owain J. Bryant**: Conceptualization, Data curation, Investigation, Formal analysis,
468 Methodology, Visualisation, Writing – original draft, Writing – review & editing.
469 **Paraminder Dhillon**: Conceptualization, Data curation, Investigation, Formal
470 analysis, Methodology, Visualisation, Writing – review & editing. **Colin Hughes**:
471 Conceptualization, Data curation, Formal analysis, Funding acquisition,
472 Investigation, Methodology, Project administration, Resources, Supervision,
473 Visualisation, Writing – review & editing. **Gillian M. Fraser**: Conceptualization, Data
474 curation, Formal analysis, Funding acquisition, Investigation, Methodology, Project
475 administration, Resources, Supervision, Visualisation, Writing – original draft, Writing
476 – review & editing.

477

478 **Acknowledgements**

479 This work was funded by grants from the Biotechnology and Biological Sciences
480 Research Council (BB/M007197/1) to G.M.F, the Wellcome Trust (082895/Z/07/Z) to
481 C.H. and G.M.F., a Biotechnology and Biological Sciences Research Council
482 studentship to P.D., and a University of Cambridge John Lucas Walker studentship
483 to O.J.B.

484

485 **Competing interests**

486 The authors declare no competing interests.

487

488 **Materials & Correspondence**

489 Materials are available from the corresponding author upon request.

490 **References**


491 [1] L. D. B. Evans, C. Hughes, and G. M. Fraser, “Building a flagellum in biological
492 outer space.,” *Microb. cell (Graz, Austria)*, 2014.

493 [2] W. Deng *et al.*, “Assembly, structure, function and regulation of type III
494 secretion systems,” *Nature Reviews Microbiology*. 2017.

495 [3] D. Büttner and S. Y. He, “Type III protein secretion in plant pathogenic
496 bacteria,” *Plant Physiol.*, 2009.

497 [4] M. E. Konkel *et al.*, “Secretion of virulence proteins from Campylobacter jejuni
498 is dependent on a functional flagellar export apparatus,” *J. Bacteriol.*, 2004.

499 [5] M. Dongre *et al.*, “Flagella-mediated secretion of a novel Vibrio cholerae
500 cytotoxin affecting both vertebrate and invertebrate hosts,” *Commun. Biol.*,
501 2018.

502 [6] L. D. B. Evans, C. Hughes, and G. M. Fraser, “Building a flagellum outside the
503 bacterial cell,” *Trends in Microbiology*. 2014.

504 [7] T. Minamino and K. Namba, “Distinct roles of the FliI ATPase and proton
505 motive force in bacterial flagellar protein export,” *Nature*, vol. 451, no. 7177,
506 pp. 485–488, 2008.

507 [8] K. Paul, M. Erhardt, T. Hirano, D. F. Blair, and K. T. Hughes, “Energy source of
508 flagellar type III secretion,” *Nature*, 2008.

509 [9] A. W. Williams, S. Yamaguchi, F. Togashi, S. I. Aizawa, I. Kawagishi, and R.
510 M. Macnab, “Mutations in fliK and flhB affecting flagellar hook and filament
511 assembly in Salmonella typhimurium,” *J. Bacteriol.*, 1996.

512 [10] G. M. Fraser, T. Hirano, H. U. Ferris, L. L. Devgan, M. Kihara, and R. M.
513 Macnab, “Substrate specificity of type III flagellar protein export in Salmonella

514 is controlled by subdomain interactions in FlhB.," *Mol. Microbiol.*, 2003.
515 [11] G. Kuwajima, I. Kawagishi, M. Homma, J. Asaka, E. Kondo, and R. M.
516 Macnab, "Export of an N-terminal fragment of Escherichia coli flagellin by a
517 flagellum-specific pathway.," *Proc. Natl. Acad. Sci.*, 2006.
518 [12] T. Minamino and R. M. Macnab, "Components of the Salmonella flagellar
519 export apparatus and classification of export substrates," *J. Bacteriol.*, 1999.
520 [13] M. G. Kornacker and A. Newton, "Information essential for cell-cycle-
521 dependent secretion of the 591-residue Caulobacter hook protein is confined
522 to a 21-amino-acid sequence near the N-terminus," *Mol. Microbiol.*, 1994.
523 [14] L. D. B. Evans, S. Poulter, E. M. Terentjev, C. Hughes, and G. M. Fraser, "A
524 chain mechanism for flagellum growth," *Nature*, vol. 504, no. 7479, pp. 287–
525 290, 2013.
526 [15] B. M. Végh, P. Gál, J. Dobó, P. Závodszky, and F. Vonderviszt, "Localization
527 of the flagellum-specific secretion signal in Salmonella flagellin," *Biochem.*
528 *Biophys. Res. Commun.*, 2006.
529 [16] P. Wattiau, B. Bernier, P. Deslée, T. Michiels, and G. R. Cornelis, "Individual
530 chaperones required for Yop secretion by Yersinia," *Proc. Natl. Acad. Sci. U.*
531 *S. A.*, 1994.
532 [17] G. M. Fraser, J. C. Q. Bennett, and C. Hughes, "Substrate-specific binding of
533 hook-associated proteins by FlgN and FliT, putative chaperones for flagellum
534 assembly," *Mol. Microbiol.*, vol. 32, no. 3, pp. 569–580, 1999.
535 [18] J. Thomas, G. P. Stafford, and C. Hughes, "Docking of cytosolic chaperone-
536 substrate complexes at the membrane ATPase during flagellar type III protein
537 export.," *Proc. Natl. Acad. Sci. U. S. A.*, vol. 101, no. 11, pp. 3945–3950, 2004.

538 [19] Y. Akeda and J. E. Galán, “Chaperone release and unfolding of substrates in
539 type III secretion,” *Nature*, 2005.
540 [20] G. Bange, N. Kümmerer, C. Engel, G. Bozkurt, K. Wild, and I. Sinning, “FlhA
541 provides the adaptor for coordinated delivery of late flagella building blocks to
542 the type III secretion system.,” *Proc. Natl. Acad. Sci. U. S. A.*, vol. 107, no. 25,
543 pp. 11295–11300, 2010.
544 [21] M. Kinoshita, N. Hara, K. Imada, K. Namba, and T. Minamino, “Interactions of
545 bacterial flagellar chaperone-substrate complexes with FlhA contribute to co-
546 ordinating assembly of the flagellar filament,” *Mol. Microbiol.*, vol. 90, no. 6, pp.
547 1249–1261, 2013.
548 [22] L. Kuhlen *et al.*, “Structure of the core of the type iii secretion system export
549 apparatus,” *Nat. Struct. Mol. Biol.*, 2018.
550 [23] P. Abrusci *et al.*, “Architecture of the major component of the type III secretion
551 system export apparatus,” *Nat. Struct. Mol. Biol.*, vol. 20, no. 1, pp. 99–104,
552 2012.
553 [24] K. Eichelberg, C. C. Ginocchio, and J. E. Galan, “Molecular and functional
554 characterization of the Salmonella typhimurium invasion genes invB and invC:
555 Homology of InvC to the F0F1 ATPase family of proteins,” *J. Bacteriol.*, 1994.
556 [25] S. Johnson, L. Kuhlen, J. C. Deme, P. Abrusci, and S. M. Lea, “The Structure
557 of an Injectisome Export Gate Demonstrates Conservation of Architecture in
558 the Core Export Gate between Flagellar and Virulence Type III Secretion
559 Systems,” *MBio*, 2019.
560 [26] Q. Xing, K. Shi, A. Portaliou, P. Rossi, A. Economou, and C. G. Kalodimos,
561 “Structures of chaperone-substrate complexes docked onto the export gate in

562 a type III secretion system," *Nat. Commun.*, 2018.
563 [27] C. Butan, M. Lara-Tejero, W. Li, J. Liu, and J. E. Galán, "High-resolution view
564 of the type III secretion export apparatus in situ reveals membrane remodeling
565 and a secretion pathway.," *Proc. Natl. Acad. Sci. U. S. A.*, 2019.
566 [28] S. Mizuno, H. Amida, N. Kobayashi, S. I. Aizawa, and S. I. Tate, "The NMR
567 structure of FliK, the trigger for the switch of substrate specificity in the flagellar
568 type III secretion apparatus," *J. Mol. Biol.*, 2011.
569 [29] E. Ward, T. T. Renault, E. A. Kim, M. Erhardt, K. T. Hughes, and D. F. Blair,
570 "Type-III secretion pore formed by flagellar protein FliP," *Mol. Microbiol.*, 2018.
571 [30] L. Kuhlen *et al.*, "The substrate specificity switch FlhB assembles onto the
572 export gate to regulate type three secretion," *Nat. Commun.*, 2020.
573 [31] V. A. Meshcheryakov, A. Kitao, H. Matsunami, and F. A. Samatey, "Inhibition
574 of a type III secretion system by the deletion of a short loop in one of its
575 membrane proteins," *Acta Crystallogr. Sect. D Biol. Crystallogr.*, 2013.
576 [32] F. Vonderviszt, R. Ishima, K. Akasaka, and S. I. Aizawa, "Terminal disorder: A
577 common structural feature of the axial proteins of bacterial flagellum?," *J. Mol.*
578 *Biol.*, 1992.
579 [33] C. Weber-Sparenberg *et al.*, "Characterization of the type III export signal of
580 the flagellar hook scaffolding protein FlgD of Escherichia coli," *Arch. Microbiol.*,
581 2006.
582 [34] S. I. Aizawa, F. Vonderviszt, R. Ishima, and K. Akasaka, "Termini of
583 Salmonella flagellin are disordered and become organized upon
584 polymerization into flagellar filament," *J. Mol. Biol.*, 1990.
585 [35] A. Tsirigotaki, J. De Geyter, N. Šoštarić, A. Economou, and S. Karamanou,

586 "Protein export through the bacterial Sec pathway," *Nature Reviews*
587 *Microbiology*. 2017.
588 [36] T. Palmer and B. C. Berks, "The twin-arginine translocation (Tat) protein export
589 pathway," *Nature Reviews Microbiology*. 2012.
590 [37] T. Hirano, S. Shibata, K. Ohnishi, T. Tani, and S. I. Aizawa, "N-terminal signal
591 region of FliK is dispensable for length control of the flagellar hook," *Mol.*
592 *Microbiol.*, 2005.
593 [38] T. Minamino, B. González-Pedrajo, K. Yamaguchi, S. I. Aizawa, and R. M.
594 Macnab, "FliK, the protein responsible for flagellar hook length control in
595 Salmonella, is exported during hook assembly," *Mol. Microbiol.*, 1999.
596 [39] J. Thomas, G. P. Stafford, and C. Hughes, "Docking of cytosolic chaperone-
597 substrate complexes at the membrane ATPase during flagellar type III protein
598 export," *Proc. Natl. Acad. Sci.*, 2004.
599 [40] T. Ibuki, Y. Uchida, Y. Hironaka, K. Namba, K. Imada, and T. Minamino,
600 "Interaction between FliJ and FlhA, components of the bacterial flagellar type iii
601 export apparatus," *J. Bacteriol.*, 2013.
602 [41] M. San Miguel, R. Marrington, P. M. Rodger, A. Rodger, and C. Robinson, "An
603 Escherichia coli twin-arginine signal peptide switches between helical and
604 unstructured conformations depending on the hydrophobicity of the
605 environment," *Eur. J. Biochem.*, 2003.
606 [42] M. Erhardt *et al.*, "Mechanism of type-III protein secretion: Regulation of FlhA
607 conformation by a functionally critical charged-residue cluster," *Mol. Microbiol.*,
608 vol. 104, no. 2, pp. 234–249, 2017.
609 [43] R. Zarivach *et al.*, "Structural analysis of the essential self-cleaving type III

610 secretion proteins EscU and SpaS," *Nature*, 2008.

611 [44] G. T. Lountos, B. P. Austin, S. Nallamsetty, and D. S. Waugh, "Atomic
612 resolution structure of the cytoplasmic domain of Yersinia pestis YscU, a
613 regulatory switch involved in type III secretion," *Protein Sci.*, 2009.

614 [45] A. Aunkham *et al.*, "Structural basis for chitin acquisition by marine Vibrio
615 species," *Nat. Commun.*, 2018.

616 [46] Y. Ge, A. Draycheva, T. Bornemann, M. V. Rodnina, and W. Wintermeyer,
617 "Lateral opening of the bacterial translocon on ribosome binding and signal
618 peptide insertion," *Nat. Commun.*, 2014.

619 [47] J. Zimmer, Y. Nam, and T. A. Rapoport, "Structure of a complex of the ATPase
620 SecA and the protein-translocation channel," *Nature*, 2008.

621 [48] R. M. Voorhees, I. S. Fernández, S. H. W. Scheres, and R. S. Hegde,
622 "Structure of the mammalian ribosome-Sec61 complex to 3.4 Å resolution,"
623 *Cell*, 2014.

624 [49] H. Mori and K. Cline, "A twin arginine signal peptide and the pH gradient
625 trigger reversible assembly of the thylakoid ΔpH/Tat translocase," *J. Cell Biol.*,
626 2002.

627 [50] L. D. B. Evans, P. M. Bergen, O. J. Bryant, and G. M. Fraser, "Interactions of
628 flagellar structural subunits with the membrane export machinery," in *Methods
629 in Molecular Biology*, 2017.

630 [51] P. M. Bergen, "Characterisation of the structure and function of the Salmonella
631 flagellar export gate protein , FlhB .," no. September, 2017.

632 [52] F. H. Login and H. Wolf-Watz, "YscU/FlhB of Yersinia pseudotuberculosis
633 harbors a C-terminal type III secretion signal," *J. Biol. Chem.*, 2015.

634 [53] S. Frost, O. Ho, F. H. Login, C. F. Weise, H. Wolf-Watz, and M. Wolf-Watz,
635 "Autoproteolysis and Intramolecular Dissociation of Yersinia YscU Precedes
636 Secretion of Its C-Terminal Polypeptide YscUCC," *PLoS One*, 2012.
637 [54] T. Minamino, Y. V. Morimoto, N. Hara, and K. Namba, "An energy transduction
638 mechanism used in bacterial flagellar type III protein export," *Nat. Commun.*,
639 2011.
640 [55] M. Baba *et al.*, "Rotation of artificial rotor axles in rotary molecular motors,"
641 *Proc. Natl. Acad. Sci.*, 2016.
642 [56] N. Hara, K. Namba, and T. Minamino, "Genetic characterization of conserved
643 charged residues in the bacterial flagellar type III export protein FlhA," *PLoS*
644 *One*, vol. 6, no. 7, 2011.
645 [57] K. A. Datsenko and B. L. Wanner, "One-step inactivation of chromosomal
646 genes in Escherichia coli K-12 using PCR products," *Proc. Natl. Acad. Sci. U.*
647 *S. A.*, 2000.
648 [58] S. Hoffmann, C. Schmidt, S. Walter, J. K. Bender, and R. G. Gerlach,
649 "Scarless deletion of up to seven methylaccepting chemotaxis genes with an
650 optimized method highlights key function of CheM in Salmonella
651 Typhimurium," *PLoS One*, 2017.
652 [59] E. Amann, B. Ochs, and K. J. Abel, "Tightly regulated tac promoter vectors
653 useful for the expression of unfused and fused proteins in Escherichia coli,"
654 *Gene*, 1988.
655 [60] B. Hu, M. Lara-Tejero, Q. Kong, J. E. Galán, and J. Liu, "In Situ Molecular
656 Architecture of the Salmonella Type III Secretion Machine," *Cell*, 2017.
657 [61] T. Minamino and R. M. Macnab, "Domain structure of Salmonella FlhB, a

658 flagellar export component responsible for substrate specificity switching," *J.*
659 *Bacteriol.*, 2000.
660
661

662 **Figure legends**

663 **Figure 1. Screening for export-defective FlgD variants**

664 **a.** Whole cell (cell) and supernatant (sec) proteins from late exponential phase
665 cultures of a *Salmonella flgD* null strain expressing wild type FlgD (FlgD) or its
666 variants (Δ2-5, Δ6-10, Δ11-15, Δ16-20, Δ21-25, Δ26-30, Δ31-35, Δ36-40, Δ41-45 or
667 Δ46-50) were separated by SDS (15%)-PAGE and analysed by immunoblotting with
668 anti-FlgD polyclonal antisera.

669 **b.** A schematic displaying the intragenic suppressor mutations within amino acids 1-
670 40 of FlgD isolated from the FlgDΔ2-5 variant. Small non-polar residues are
671 highlighted in orange. All suppressor mutations were located between the gate-
672 recognition motif (GRM, blue) and the extreme N-terminus, and can be separated
673 into two classes: insertions or duplications that introduced additional sequence
674 between valine-15 and the gate-recognition motif, or missense mutations that re-
675 introduce small non-polar residues at the N-terminus.

676 **c**. Whole cell (cell) and supernatant (sec) proteins from late exponential-phase
677 cultures of *Salmonella flgD* null strains expressing suppressor mutants isolated from
678 the FlgDΔ2-5 variant (FlgDΔ2-5-$N_8$I or FlgDΔ2-5-$T_{11}$I), FlgDΔ2-5 variant (-) or wild
679 type FlgD (FlgD) were separated by SDS (15%)-PAGE and analysed by
680 immunoblotting with anti-FlgD polyclonal antisera.

681 **d.** Whole cell (cell) and supernatant (sec) proteins from late exponential phase
682 cultures of *Salmonella flgD* null strains expressing wild type FlgD (FlgD), FlgDΔ2-5
683 (DΔ2-5) or variants of FlgDΔ2-5 containing between residues 19 and 20 a six-
684 residue insertion of either small non-polar (AGAGAG) residues (3x(AG)), polar

685 (STSTST) residues (3x(ST)), or the sequence from an isolated insertion suppressor
686 mutant (GSGSMT), were separated by SDS (15%)-PAGE and analysed by
687 immunoblotting with anti-FlgD polyclonal antisera.

688

689 **Figure 2. Export of FlgD variants in which the position of the N-terminal**
690 **hydrophobic export signal is varied relative to the gate recognition motif**
691 **(GRM)**

692 Whole cell (cell) and supernatant (sec) proteins from late exponential-phase cultures
693 of a *Salmonella flgD* null strain expressing suppressor mutants isolated from the
694 FlgDΔ2-5-$^{19}$(GSGSMT)$^{20}$-$V_{15}A$ variant ($V_{15}A$-$M_7I$, $V_{15}A$-$D_9A$, $V_{15}A$-$T_{11}I$, $V_{15}A$-$G_{14}V$),
695 their parent FlgD variant FlgDΔ2-5-$^{19}$(GSGSMT)$^{20}$-$V_{15}A$ (labelled as $V_{15}A$), FlgDΔ2-
696 5-$^{19}$(GSGSMT)$^{20}$ (labelled as -) or wild type FlgD (FlgD) were separated by SDS
697 (15%)-PAGE and analysed by immunoblotting with anti-FlgD polyclonal antisera.
698 Swimming motility (bottom panel; 0.25% soft tryptone agar) of the same strains was
699 assayed at 37ºC for 4-6 hours.

700 **b**. Whole cell (cell) and supernatant (sec) proteins from late exponential-phase
701 cultures of a *Salmonella flgD* null strain expressing wild type FlgD (FlgD), FlgDΔ9-32
702 or its variants in which residues 9-32 were replaced by between one and four six-
703 residue repeats of Gly-Ser-Thr-Asn-Ala-Ser (Δ9-32 4xRpt, Δ9-32 3xRpt, Δ9-32
704 2xRpt or Δ9-32 1xRpt) were separated by SDS (15%)-PAGE and analysed by
705 immunoblotting with anti-FlgD polyclonal antisera. Swimming motility (bottom panel;
706 0.25% soft tryptone agar) of the same strains was assayed at 37ºC for 4-6 hours.

707 **c**. Whole cell (cell) and supernatant (sec) proteins from late exponential-phase
708 cultures of a *Salmonella flgD* null strain expressing wild type FlgD (FlgD), a FlgD
709 variant in which residues 9-32 were replaced by two repeats of a six-residue
710 sequence Gly-Ser-Thr-Asn-Ala-Ser (labelled as 2xRpt) or its variants containing
711 between one and five additional residues inserted directly after the two repeats
712 (2xRpt+1, 2xRpt+2, 2xRpt+3, 2xRpt+4 or 2xRpt+5) were separated by SDS (15%)-
713 PAGE and analysed by immunoblotting with anti-FlgD polyclonal antisera. Swimming
714 motility (bottom panel; 0.25% soft tryptone agar) of the same strains was assayed at
715 37ºC for 4-6 hours.

716 **d**. Whole cell (cell) and supernatant (sec) proteins from late exponential-phase
717 cultures of a *Salmonella flgD* null strain expressing wild type FlgD (FlgD), a FlgD
718 variant in which residues 9-32 were replaced by two repeats of a six-residue
719 sequence Gly-Ser-Thr-Asn-Ala-Ser ($FlgD_{short}$) or suppressor mutants isolated from
720 this strain (rev1, rev2 or rev3) were separated by SDS (15%)-PAGE and analysed by
721 immunoblotting with anti-FlgD polyclonal antisera. Swimming motility (bottom panel;
722 0.25% soft tryptone agar) of the same strains were was assayed at 37ºC for 4-6
723 hours.

724 **e**. N-terminal sequences of wild type FlgD, a FlgD variant in which residues 9-32 are
725 replaced by two repeats of a six-residue sequence Gly-Ser-Thr-Asn-Ala-Ser (yellow;
726 $FlgD_{short}$) and its suppressor mutant revertants (rev 1-3) aligned at the gate
727 recognition motif (GRM, blue). Suppressor mutants contained insertions (underlined)
728 that introduced additional residues between the N-terminal hydrophobic signal
729 (orange) and the gate recognition motif (blue).

730

731 **Figure 3. Effect of the relative position of the N-terminus and GRM on the**

732 **export of rod and hook subunits**

733 **a.** Schematic representation of a wild type subunit (subunit$_{wild\ type}$), a subunit

734 containing a deletion of sequence between the N-terminus and GRM (subunit$_{short}$)

735 and a subunit in which the deleted sequence was replaced by four repeats of a six-

736 residue sequence Gly-Ser-Thr-Asn-Ala-Ser (yellow, subunit$_{short}$+4Rpt).

737 **b**. Whole cell (cell) and supernatant (sec) proteins from late exponential-phase

738 cultures of a *Salmonella flgE* null strain expressing wild type FlgG (FlgG$_{wild\ type}$), a

739 FlgG variant in which residues 11-35 were deleted (FlgG$_{short}$) or a FlgG variant in

740 which residues 11-35 were replaced by four repeats of a six-residue sequence Gly-

741 Ser-Thr-Asn-Ala-Ser (FlgG$_{short}$+4Rpt). All FlgG variants were engineered to contain

742 an internal 3xFLAG tag for immunodetection. Proteins were separated by SDS

743 (15%)-PAGE and analysed by immunoblotting with anti-FLAG monoclonal antisera.

744 Swimming motility (bottom panel; 0.25% soft tryptone agar) of the same strains was

745 assayed at 37ºC for 4-6 hours.

746 **c**. Whole cell (cell) and supernatant (sec) proteins from late exponential-phase

747 cultures of a *Salmonella flgD* null strain expressing wild type FlgE (FlgE$_{wild\ type}$), a

748 FlgE variant in which residues 9-32 were deleted (FlgE$_{short}$) or a FlgE variant in which

749 residues 9-32 were replaced by four repeats of a six-residue sequence Gly-Ser-Thr-

750 Asn-Ala-Ser (FlgE$_{short}$+4Rpt). All FlgE variants were engineered to contain an

751 internal 3xFLAG tag for immunodetection. Proteins were separated by SDS (15%)-

752 PAGE and analysed by immunoblotting with anti-FLAG monoclonal antisera.
753 Swimming motility (bottom panel; 0.25% soft tryptone agar) of the same strains was
754 assayed at 37ºC for 4-6 hours.

755 **Figure 4. Effect on subunit export of overexpression of FlgDΔ2-5 and variants.**

756 **a.** Schematic representation of a FlgD subunit containing a N-terminal hydrophobic
757 signal (orange, 2-5) and a gate-recognition motif (blue, GRM).

758 **b.** Swimming motility of a *Salmonella* Δ*recA* strain expressing wild type FlgD (FlgD),
759 its variants (DΔ2-5ΔGRM, DΔ2-5 or DΔGRM) or empty pTrc99a vector (-). Motility
760 was assessed in 0.25% soft-tryptone agar containing 100 µg/ml ampicillin and
761 100µM IPTG and incubated for 4-6 hours at 37°C.

762

763 **c.** Whole cell (cell) and secreted proteins (secreted) from late-exponential-phase
764 cultures were separated by SDS (15%)-PAGE and analysed by immunoblotting with
765 anti-FliK, anti-FlgK, anti-FlgL, anti-FlhA or anti-FlgN polyclonal antisera. Apparent
766 molecular weights are in kilodaltons (kDa).

767 **d**. A model depicting a FlgDΔ2-5 subunit (left) docked *via* its gate recognition motif
768 (GRM, blue) at the subunit binding pocket on $FlhB_C$ (PDB: 3B0Z[31], red), preventing
769 wild type subunits (right) from docking at $FlhB_C$.

770

771

772 **Figure 5. Effect on subunit export of overexpressed $FlgE_{short}$, $FlgD_{short}$ and**
773 **variants**

774 **a.** Swimming motility of a *Salmonella* Δ*recA* strain expressing wild type FlgE (FlgE
775 wild type), a FlgE variant in which residues 9-32 were deleted ($FlgE_{short}$), a FlgE
776 variant in which residues 9-32 and residues 39-43 (corresponding to the gate-
777 recognition motif) were deleted ($FlgE_{short}$ΔGRM), a FlgE variant in which residues
778 39-43 were deleted (FlgEΔGRM) or empty pTrc99a vector (-). All FlgG variants were
779 engineered to contain an internal 3xFLAG tag for immunodetection. Motility was
780 assessed in 0.25% soft-tryptone agar containing 100 µg/ml ampicillin and 100 µM
781 IPTG and incubated for 4-6 hours at 37°C (top panel). Whole cell (cell) and secreted
782 proteins (secreted) from late-exponential-phase cultures were separated by SDS
783 (15%)-PAGE and analysed by immunoblotting with anti-FLAG monoclonal antisera
784 or anti-FlgD, anti-FliD, anti-FlgK, anti-FliK, anti-FlhA or anti-FlgN polyclonal antisera
785 (bottom). Apparent molecular weights are in kilodaltons (kDa).

786 **b.** Swimming motility of a *Salmonella* Δ*recA* strain expressing wild type FlgD (FlgD
787 wild type), a FlgD variant in which residues 9-32 were replaced with two repeats of
788 the six amino acid sequence Gly-Ser-Thr-Asn-Ala-Ser ($FlgD_{short}$), a FlgD variant in
789 which residues 9-32 were replaced with two repeats of the six amino acid sequence
790 Gly-Ser-Thr-Asn-Ala-Ser and residues 36-40 were deleted ($FlgD_{short}$ΔGRM), a FlgD
791 variant in which residues 36-40 were deleted (FlgDΔGRM) or empty pTrc99a vector
792 (-). Motility was assessed in 0.25% soft-tryptone agar containing 100 µg/ml ampicillin
793 and 100 µM IPTG and incubated for 4-6 hours at 37°C (top panel). Whole cell (cell)
794 and secreted proteins (secreted) from late-exponential-phase cultures were

795 separated by SDS (15%)-PAGE and analysed by immunoblotting with anti-FlgD,
796 anti-FliD, anti-FlgK, anti-FliK, anti-FlhA or anti-FlgN polyclonal antisera (bottom).
797 Apparent molecular weights are in kilodaltons (kDa).

798 **Figure 6. Suppression of the $FlgD_{short}$ motility defect by mutations in FliP**

799 **a**. A model depicting subunits docked *via* their gate-recognition motif (GRM, blue) at
800 the subunit binding pocket on $FlhB_C$ (PDB: 3B0Z [31], red) with N-termini of early
801 flagellar subunits adopting either an α-helical conformation separating the N-terminal
802 hydrophobic signal (2-5, orange) and gate-recognition motif (GRM, blue) by ~40-60
803 Ångstrom (where each amino acid is on average separated by ~1.5Å, left) or an
804 unfolded conformation where the polypeptide contour length separating the N-
805 terminal hydrophobic signal (2-5) and gate-recognition motif (GRM) is ~90-150
806 Ångstrom (where each amino acid is on average separated by ~3.5Å, middle left).
807 Values corresponding to the distance separating the N-terminal hydrophobic signal
808 (2-5, orange) and gate-recognition motif (GRM, blue) of a FlgD subunit variant in
809 which residues 9-32 are replaced with two repeats of the six amino acid sequence
810 Gly-Ser-Thr-Asn-Ala-Ser ($FlgD_{short}$) indicate that the N-terminal hydrophobic signal
811 (2-5, orange) and gate-recognition motif (GRM, blue) are separated by ~29
812 Ångstrom (α-helical conformation, middle right) or ~67 Ångstrom (unfolded
813 polypeptide contour length, right).

814 **b.** Placement of the crystal structure of FlhBc (PDB:3BOZ [31]; red) and the cryo-EM
815 structure of FliPQR-FlhB (PDB:6S3L[30]) in a tomographic reconstruction of the
816 *Salmonella* SPI-1 injectisome (EMD-8544 [60]; grey). The minimum distance
817 between the subunit gate recognition motif binding site on $FlhB_C$ (grey) to $FlhB_N$

818 (defined as *Salmonella* FlhB residue 211 [61]; ~78Å) was estimated by combining:
819 the value corresponding to the distance between the subunit binding pocket on
820 $FlhB_C$ [14] (grey) and the N-terminal visible residue ($D_{229}$) in the $FlhB_C$ structure
821 (PDB:3BOZ [31]; ~52Å) with the value corresponding to the minimum distance
822 between FlhB residues 211 and 228 (based on a linear α-helical conformation;
823 ~26Å).

824

825 **c.** Swimming motility of recombinant *Salmonella flgD* null strains producing a
826 chromosomally-encoded FliP-$M_{210}$A variant ($M_{210}$A gate, left) or wild type FliP (wild
827 type gate, right). Wild type FliP and FliP-$M_{210}$A were engineered to contain an
828 internal HA tag positioned between residue 21 and 22 to allow immunodetection of
829 FliP. Both strains produced either a pTrc99a plasmid-encoded FlgD subunit variant
830 in which residues 9-32 were replaced with two repeats of the six amino acid
831 sequence Gly-Ser-Thr-Asn-Ala-Ser ($FlgD_{short}$; top panel) or a pTrc99a plasmid-
832 encoded wild type FlgD subunit ($FlgD_{wild\ type}$; bottom panel). Motility was assessed in
833 0.25% soft-tryptone agar containing 100 µg/ml ampicillin and 50 µM IPTG and
834 incubated for 16 hours (top panel) or 4-6 hours at 37°C (bottom panel).

835 **d.** The mean motility halo diameter of a recombinant *Salmonella flgD* null strain
836 producing chromosomally-encoded FliP-$M_{210}$A ($M_{210}$A gate, left) and expressing the
837 FlgD short variant (left hand bar) was plotted as a percentage of the mean motility
838 halo diameter of the wild type FliP gate strain (wild type) producing FlgDshort (right
839 hand bar). Error bars show the standard error of the mean calculated from four
840 biological replicates. * indicates a p-value $< 0.05$.

841 **Supplementary Figure Legends**

842 **Figure S1.**

843 **a**. N-terminal sequences of all *Salmonella* flagellar rod and hook subunits aligned at
844 their gate recognition motif (GRM, blue). Small non-polar residues upstream of the
845 gate recognition motif are highlighted (yellow).

846

847 **b**. Hydrophobicity plots for the N-terminal 60 residues of each *Salmonella* flagellar
848 rod and hook subunit were generated by ExPASy tools using the Kyte and Doolittle
849 method [62]. The *x* axis of the plot indicates the amino acid position, starting from the
850 N terminus. The *y* axis of the plot indicates the hydrophobicity of the amino acid
851 sequence, where higher values represent higher hydrophobicity. Amino acid
852 sequence corresponding to the gate-recognition motif of each subunit is highlighted
853 in blue.

854

855 **Figure S2**

856 **a**. Swimming motility of a *Salmonella* Δ*recA* strain expressing suppressor mutants
857 isolated from the FlgDΔ2-5 variant (FlgDΔ2-5 $N_8$I or FlgDΔ2-5 $T_{11}$I), the parent
858 FlgDΔ2-5 variant (DΔ2-5) or wild type FlgD (FlgD). Motility was assessed in 0.25%
859 soft-tryptone agar containing 100 µg/ml ampicillin and 50 µM IPTG and incubated 4-
860 6 hours at 37°C.

861

862 **b**. Swimming motility of a *Salmonella* Δ*recA* strain expressing wild type FlgD (FlgD),
863 FlgDΔ2-5 (DΔ2-5) or its variants containing a six-residue insertion between residues
864 19 and 20 of either small non-polar (AGAGAG) residues (DΔ2-5 3x(AG)), polar

865 (STSTST) residues (DΔ2-5 3x(ST)), or the sequence from an isolated insertion
866 suppressor mutant (GSGSMT) (DΔ2-5 GSGSMT). Motility was assessed in 0.25%
867 soft-tryptone agar containing 100 µg/ml ampicillin and 50 µM IPTG and incubated 4-
868 6 hours at 37°C.
869
870 **Figure S3**
871 **a**. Whole cell (cell) and supernatant (secreted) proteins from late exponential-phase
872 cultures of *Salmonella flgD* null strains expressing: suppressor mutants isolated from
873 the FlgDΔ2-5 variant (FlgDΔ2-5 $N_8$I or FlgDΔ2-5 $T_{11}$I), FlgDΔ2-5 variant (-) or wild
874 type FlgD (FlgD) were separated by SDS (15%)-PAGE and analysed by
875 immunoblotting with anti-FlhA or FlgN polyclonal antisera. Apparent molecular
876 weights are in kilodaltons (kDa).
877
878 **b**. Whole cell (cell) and supernatant (secreted) proteins from late exponential-phase
879 cultures of *Salmonella flgD* null strains expressing wild type FlgD (FlgD), FlgDΔ2-5
880 (DΔ2-5) or its variants containing a six-residue insertion between residues 19 and 20
881 of either small non-polar (AGAGAG) residues (DΔ2-5 3x(AG)), polar (STSTST)
882 residues (DΔ2-5 3x(ST)), or the sequence from an isolated insertion suppressor
883 mutant (GSGSMT) (DΔ2-5 GSGSMT) were separated by SDS (15%)-PAGE and
884 analysed by immunoblotting with anti-FlgD polyclonal antisera. Apparent molecular
885 weights are in kilodaltons (kDa).
886
887
888

889 **Figure S4**

890 **a**. Whole cell (cell) and supernatant (secreted) proteins from late exponential-phase
891 cultures of a *Salmonella flgD* null strain expressing suppressor mutants isolated from
892 a FlgDΔ2-5-$^{19}$(GSGSMT)$^{20}$-$V_{15}A$ variant ($V_{15}A$-$M_7I$, $V_{15}A$-$D_9A$, $V_{15}A$-$T_{11}I$, $V_{15}A$-
893 $G_{14}V$), their parent FlgD variant FlgDΔ2-5-$^{19}$(GSGSMT)$^{20}$-$V_{15}A$ ($V_{15}A$), FlgDΔ2-5-
894 $^{19}$(GSGSMT)$^{20}$ (-) or wild type FlgD (FlgD) were separated by SDS (15%)-PAGE
895 and analysed by immunoblotting with anti-FlhA and FlgN polyclonal antisera.
896 Apparent molecular weights are in kilodaltons (kDa).

897

898 **Figure S5**

899 **a**. Whole cell (cell) and supernatant (secreted) proteins from late exponential-phase
900 cultures of a *Salmonella flgD* null strain expressing wild type FlgD (FlgD), FlgDΔ9-32
901 or its variants in which residues 9-32 were replaced by between one and four six-
902 residue repeats of Gly-Ser-Thr-Asn-Ala-Ser (GSTNAS): (Δ9-32 4xRpt, Δ9-32 3xRpt,
903 Δ9-32 2xRpt, Δ9-32 1xRpt) were separated by SDS (15%)-PAGE and analysed by
904 immunoblotting with anti-FlhA and anti-FlgN polyclonal antisera. Apparent molecular
905 weights are in kilodaltons (kDa).

906

907 **b**. Whole cell (cell) and supernatant (secreted) proteins from late exponential-phase
908 cultures of a *Salmonella flgD* null strain expressing wild type FlgD (FlgD), a FlgD
909 variant in which residues 9-32 were replaced by two repeats of a six-residue
910 sequence Gly-Ser-Thr-Asn-Ala-Ser (2xRpt) or its variants containing between one
911 and five additional residues inserted directly after the two repeats (2xRpt+ 1, 2xRpt+
912 2, 2xRpt+ 3, 2xRpt+ 4 or 2xRpt+ 5) were separated by SDS (15%)-PAGE and

913 analysed by immunoblotting with anti-FlgD polyclonal antisera. Apparent molecular
914 weights are in kilodaltons (kDa).
915
916 **Figure S6**
917 **a**. Whole cell (cell) and supernatant (secreted) proteins from late exponential-phase
918 cultures of a *Salmonella flgD* null strain expressing wild type FlgD (FlgD), a FlgD
919 variant in which residues 9-32 were replaced by two repeats of a six-residue
920 sequence Gly-Ser-Thr-Asn-Ala-Ser ($FlgD_{short}$) or suppressor mutants isolated from
921 this strain (rev1, rev2 or rev3) were separated by SDS (15%)-PAGE and analysed by
922 immunoblotting with anti-FlhA and anti-FlgN polyclonal antisera. Apparent molecular
923 weights are in kilodaltons (kDa).
924
925 **b**. N-terminal sequences of wild type FlgD (wild type), a FlgD variant in which residus
926 9-32 are replaced by two repeats of a six-residue sequence Gly-Ser-Thr-Asn-Ala-Ser
927 (yellow; $FlgD_{short}$) and its suppressor mutants (rev 1-7) aligned to their gate-
928 recognition motif (GRM, blue). Suppressor mutants contained insertions (underlined)
929 that introduced additional residues between the N-terminal hydrophobic signal
930 (orange) and the gate-recognition motif (blue).
931
932 **Figure S7**
933 **a**. Whole cell (cell) and supernatant (sec) proteins from late exponential-phase
934 cultures of a *Salmonella flgE* null strain expressing wild type FlgG ($FlgG_{wild\ type}$), a
935 FlgG variant in which residues 11-35 were deleted ($FlgG_{short}$) or a FlgG variant in
936 which residues 11-35 were replaced by four repeats of a six-residue sequence Gly-

937 Ser-Thr-Asn-Ala-Ser ($FlgG_{short}$+4Rpt). All FlgG variants were engineered to contain
938 an internal 3xFLAG tag for immunodetection. Proteins were separated by SDS
939 (15%)-PAGE and analysed by immunoblotting with anti-FlhA or anti-FlgN polyclonal
940 antisera. Apparent molecular weights are in kilodaltons (kDa).
941
942 **b**. Whole cell (cell) and supernatant (secreted) proteins from late exponential-phase
943 cultures of a *Salmonella flgD* null strain expressing wild type FlgE ($FlgE_{wild\ type}$), a
944 FlgE variant in which residues 9-32 were deleted ($FlgE_{short}$) or a FlgE variant in which
945 residues 9-32 were replaced by four repeats of a six-residue sequence Gly-Ser-Thr-
946 Asn-Ala-Ser ($FlgE_{short}$+4Rpt). All FlgE variants were engineered to contain an
947 internal 3xFLAG tag for immunodetection. Proteins were separated by SDS (15%)-
948 PAGE and analysed by immunoblotting with anti-FLAG monoclonal antisera.
949 Swimming motility (bottom panel; 0.25% soft tryptone agar) of the same strains were
950 carried out at 37ºC for 4-6 hours. Apparent molecular weights are in kilodaltons
951 (kDa).
952
953 **Figure S8**
954 **a**. Whole cell (cell) proteins from late exponential-phase cultures of recombinant
955 *Salmonella flgD* null strains producing a chromosomally-encoded FliP-$M_{210}$A variant
956 ($M_{210}$A gate, left) or wild type FliP (wild type gate, right). Wild type FliP and FliP-
957 $M_{210}$A were engineered to contain an internal HA tag positioned between residue 21
958 and 22 to allow immunodetection of FliP [29] (bottom panel). Both strains produced
959 either a pTrc99a plasmid-encoded FlgD subunit variant in which residues 9-32 were
960 replaced with two repeats of the six amino acid sequence Gly-Ser-Thr-Asn-Ala-Ser

961 ($FlgD_{short}$; top panel) or a pTrc99a plasmid-encoded wild type FlgD subunit ($FlgD_{wild}$

962 $_{type}$; middle panel). Proteins were separated by SDS (15%)-PAGE and analysed by

963 immunoblotting with anti-FlgD polyclonal antisera or anti-HA monoclonal antisera.

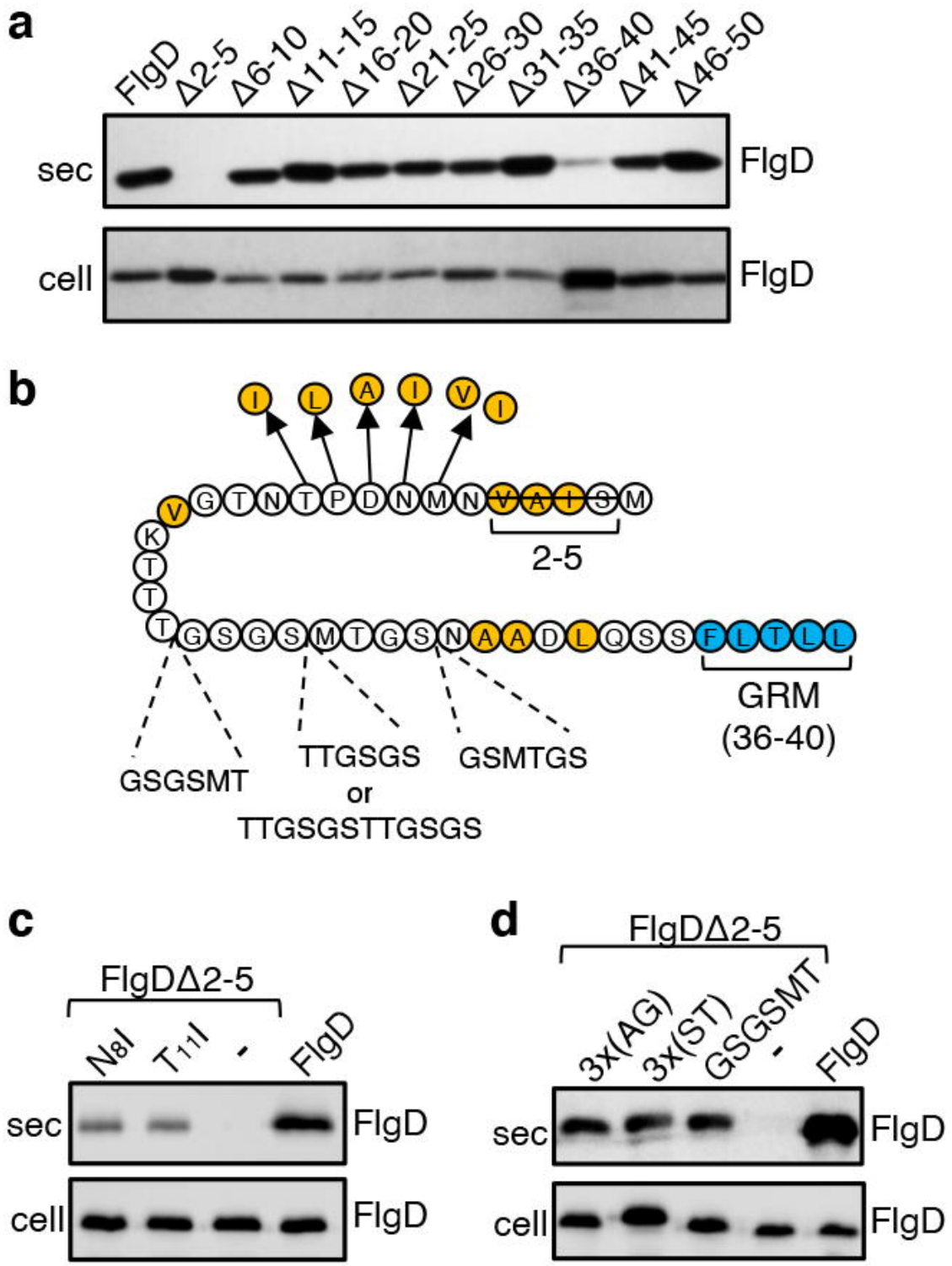
a
FlgD
Δ2-5
Δ6-10
Δ11-15
Δ16-20
Δ21-25
Δ26-30
Δ31-35
Δ36-40
Δ41-45
Δ46-50
sec
cell
FlgD
FlgD
b
I L A I V I
V G T N T P D N M N V A I S M
K T T T
T G S G S M T G S N A A D L Q S S F L T L L
2-5
GRM
(36-40)
GSGSMT
TTGSGS
or
TTGSGSTTGSGS
GSMTGS
c
FlgDΔ2-5
N8I
T11I
-
FlgD
sec
cell
FlgD
FlgD
d
FlgDΔ2-5
3x(AG)
3x(ST)
GSGSMT
-
FlgD
sec
cell
FlgD
FlgD

Figure 1

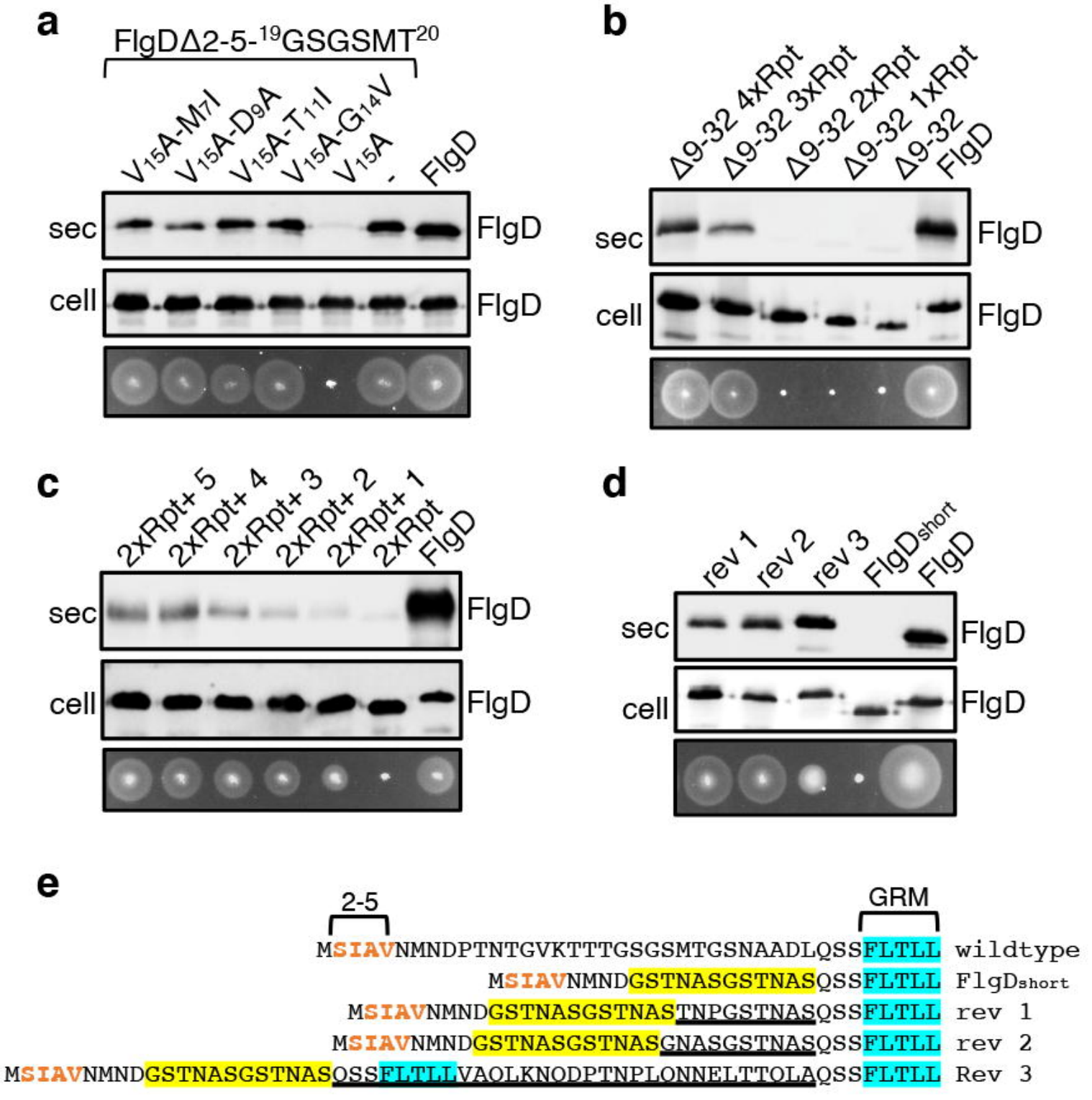
a
FlgDΔ2-5-19GSGSMT20
V15A-M7I
V15A-D9A
V15A-T11I
V15A-G14V
V15A
-
FlgD
sec
cell
FlgD
b
Δ9-32 4xRpt
Δ9-32 3xRpt
Δ9-32 2xRpt
Δ9-32 1xRpt
Δ9-32
FlgD
c
2xRpt+ 5
2xRpt+ 4
2xRpt+ 3
2xRpt+ 2
2xRpt+ 1
2xRpt
d
rev 1
rev 2
rev 3
FlgDshort
e
2-5
GRM
MSIAVNMNDPTNTGVKTTTGSGSMTGSNAADLQSSFLTLL wildtype
MSIAVNMNDGSTNASGSTNASQSSFLTLL FlgDshort
MSIAVNMNDGSTNASGSTNASTNPGSTNASQSSFLTLL rev 1
MSIAVNMNDGSTNASGSTNASGNASGSTNASQSSFLTLL rev 2
MSIAVNMNDGSTNASGSTNASQSSFLTLLVAQLKNQDPTNPLQNNELTTQLAQSSFLTLL Rev 3

Figure 2

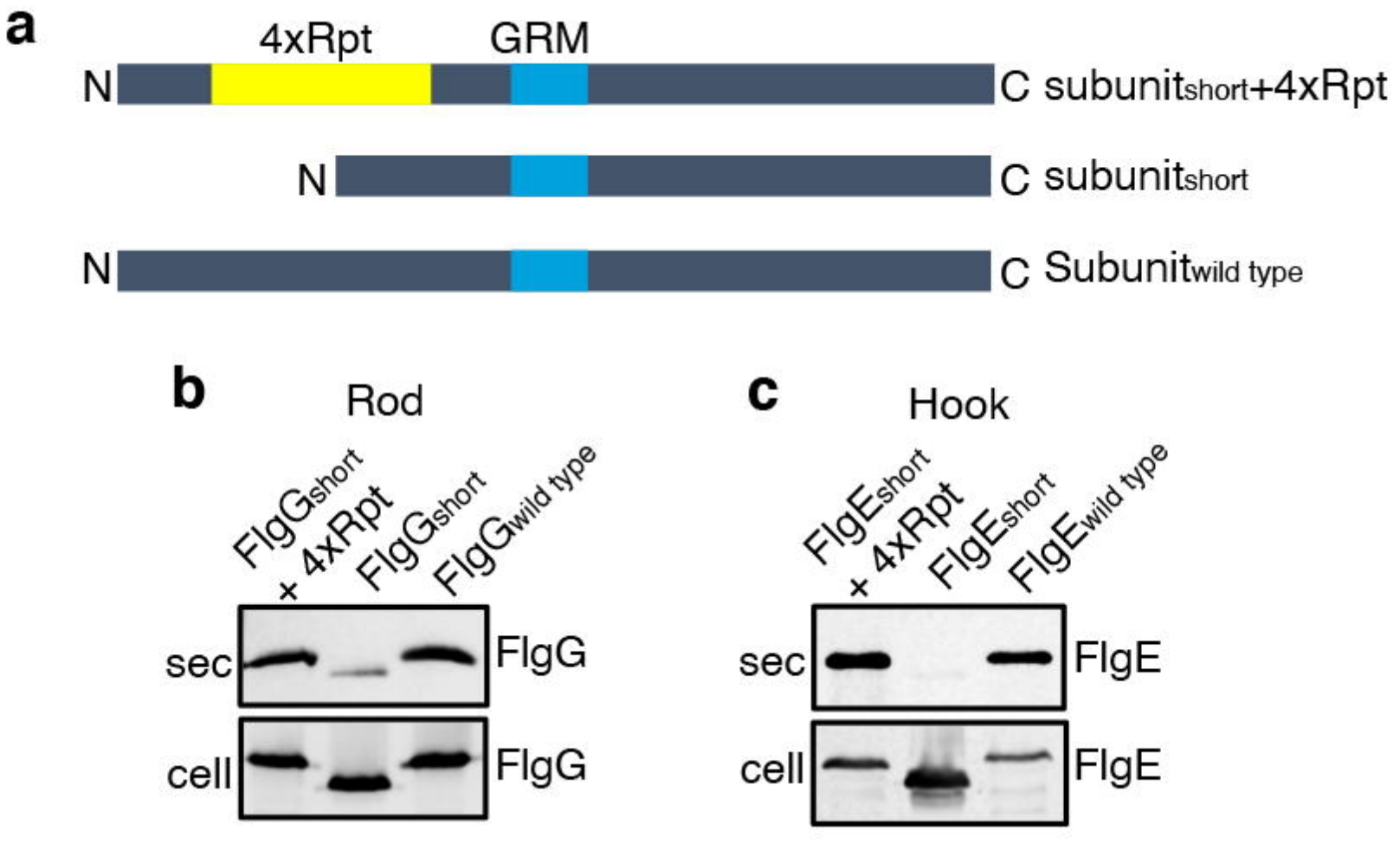
a
4xRpt
GRM
N
C subunitshort+4xRpt
N
C subunitshort
N
C Subunitwild type
b
Rod
FlgGshort + 4xRpt
FlgGshort
FlgGwild type
sec
cell
FlgG
FlgG
c
Hook
FlgEshort + 4xRpt
FlgEshort
FlgEwild type
sec
cell
FlgE
FlgE

Figure 3

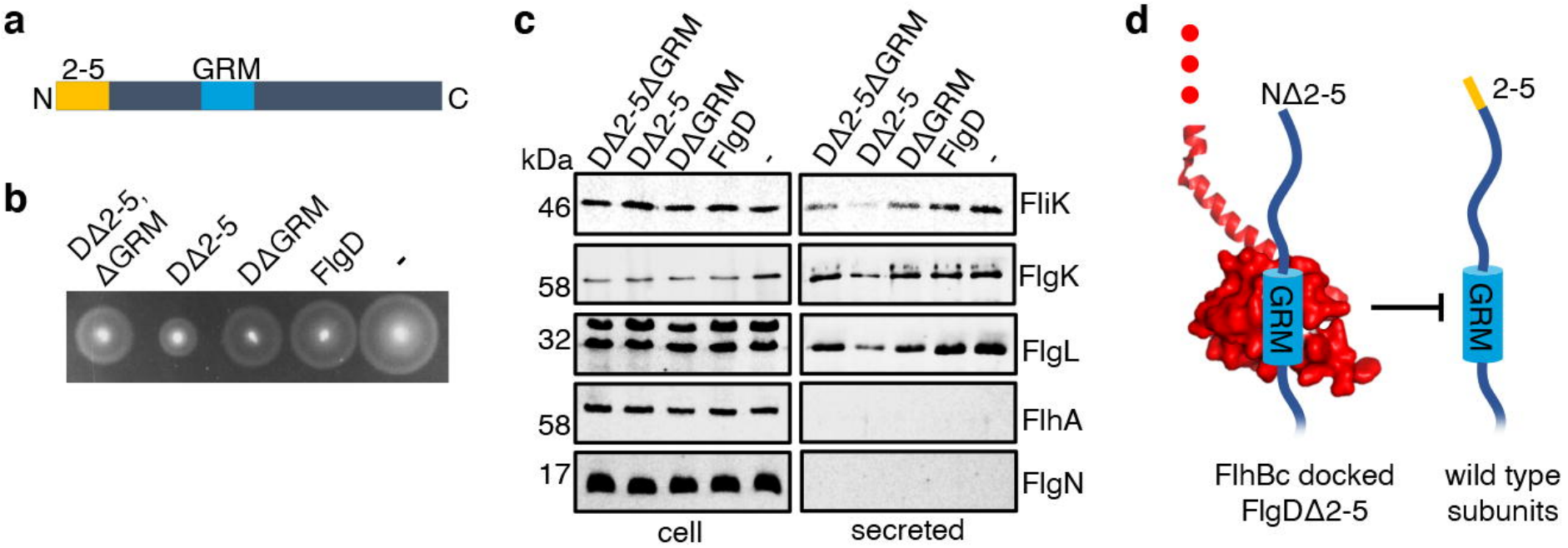
a
2-5
GRM
N
C
b
DΔ2-5, ΔGRM
DΔ2-5
DΔGRM
FlgD
-
c
kDa
DΔ2-5ΔGRM
DΔ2-5
DΔGRM
FlgD
-
46
58
32
58
17
FliK
FlgK
FlgL
FlhA
FlgN
cell
secreted
d
NΔ2-5
2-5
GRM
GRM
FlhBc docked FlgDΔ2-5
wild type subunits

Figure 4

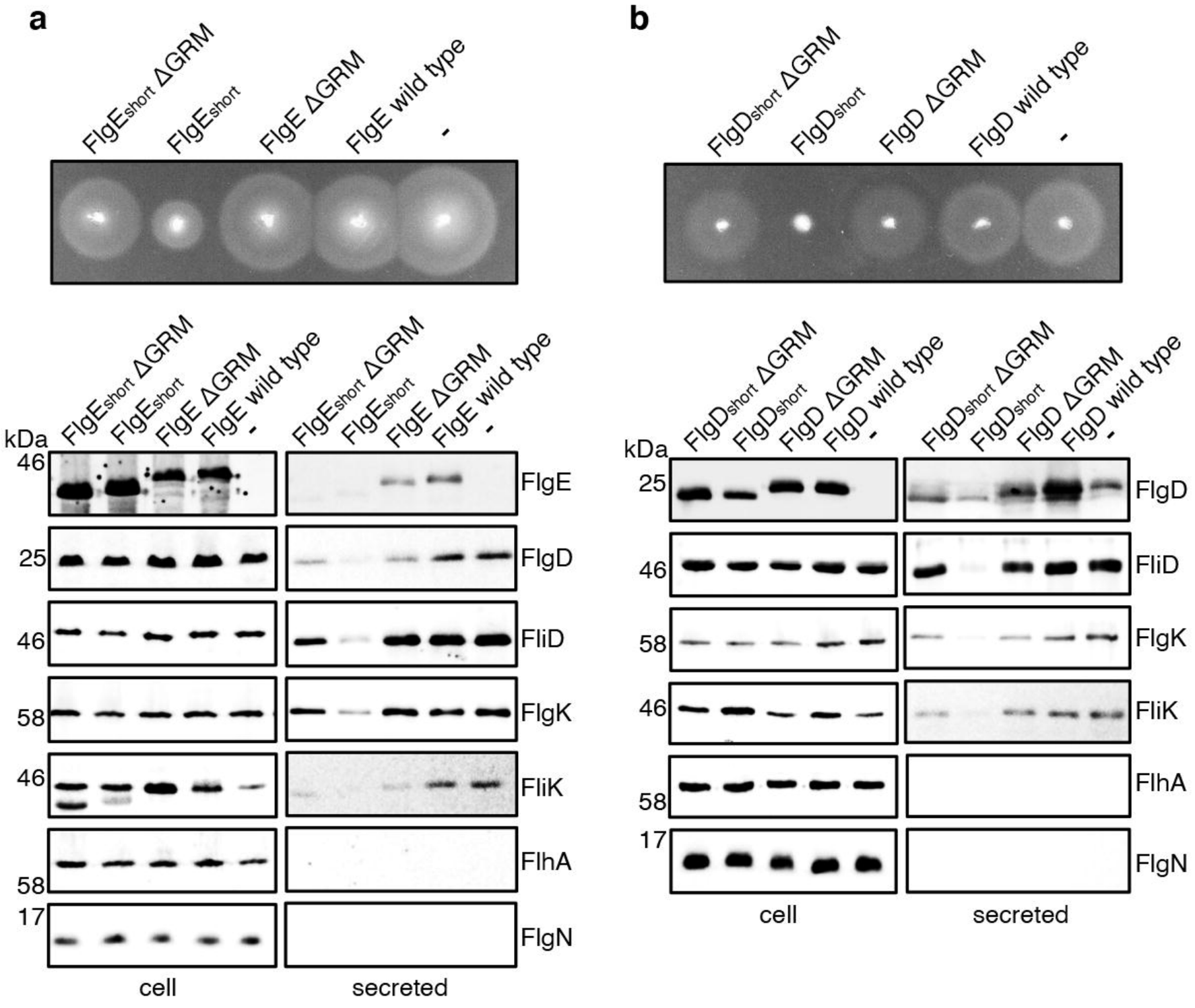
a
FlgEshort ΔGRM
FlgEshort
FlgE ΔGRM
FlgE wild type
-
kDa
46
25
46
58
46
58
17
FlgE
FlgD
FliD
FlgK
FliK
FlhA
FlgN
cell
secreted
b
FlgDshort ΔGRM
FlgDshort
FlgD ΔGRM
FlgD wild type
-
kDa
25
46
58
46
58
17
FlgD
FliD
FlgK
FliK
FlhA
FlgN
cell
secreted

Figure 5

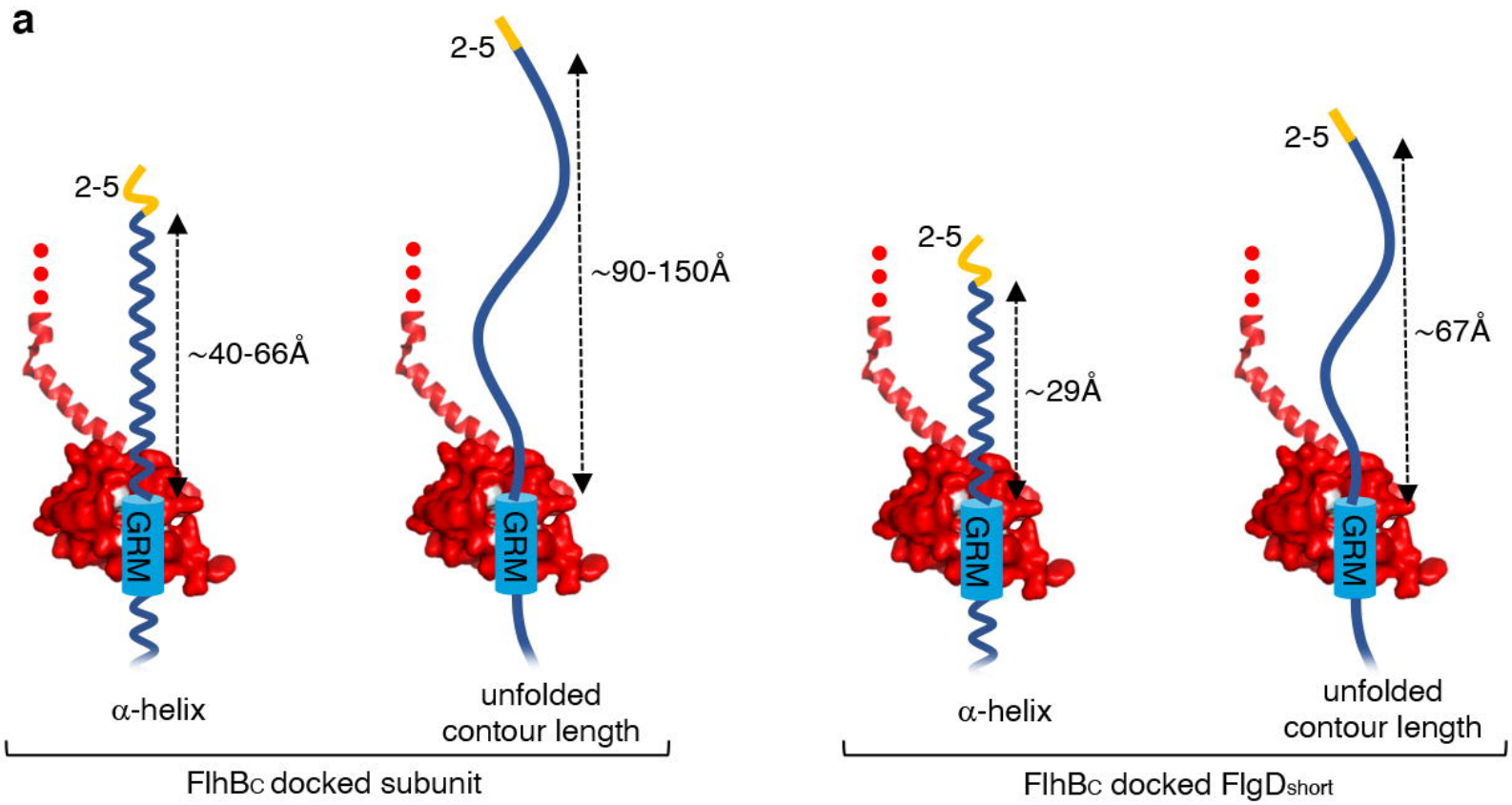
a
2-5
~40-66Å
GRM
α-helix
2-5
~90-150Å
GRM
unfolded
contour length
FlhBc docked subunit
2-5
~29Å
GRM
α-helix
2-5
~67Å
GRM
unfolded
contour length
FlhBc docked FlgDshort

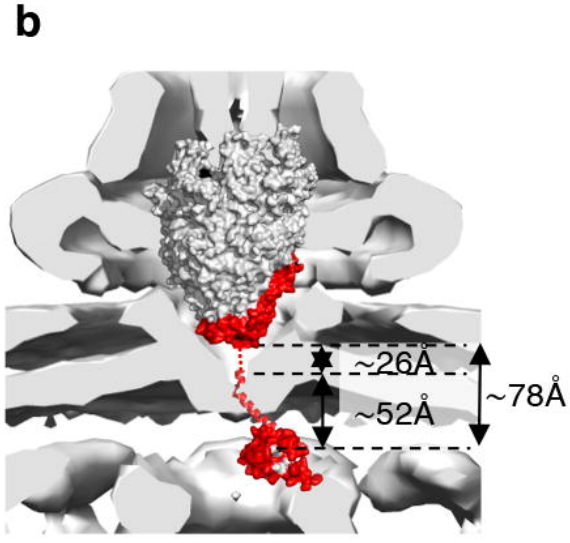
b
~26Å
~52Å
~78Å

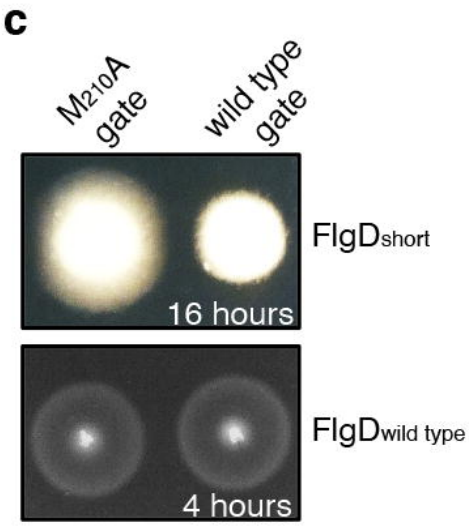
c
M210A gate
wild type gate
FlgDshort
16 hours
FlgDwild type
4 hours

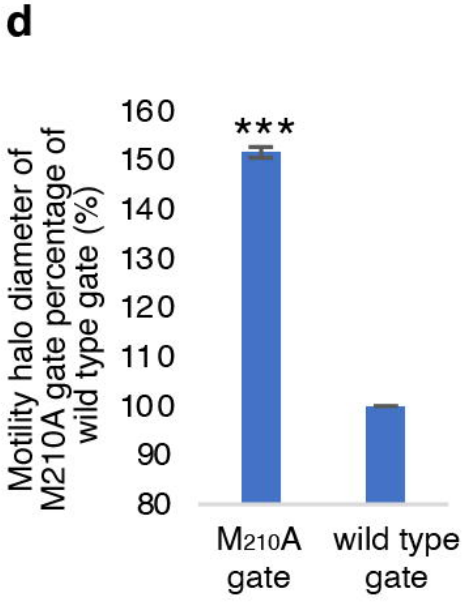
d
Motility halo diameter of M210A gate percentage of wild type gate (%)
160
150
140
130
120
110
100
90
80
***
M210A gate
wild type gate

Figure 6